

Microstructure effect on the properties of a commercial low-fusing dental porcelain

ATHENA TSETSEKOU*

*Department of Mineral Resources Engineering, Technical University of Crete, University Campus, 73100 Chania, Greece
E-mail: athtse@mred.tuc.gr*

TRIANAFILLOS PAPADOPOULOS

Department of Dental Biomaterials, Dental School, University of Athens, Thivon 2, 115 27, Athens, Greece

OTHON ADAMOPOULOS

Ceramics and Refractories Technological Development Company (CERECO S.A.), 72nd km of Athens, Lamia Ntl. Road, P.O. Box 146, 34100, Chalkida, Greece

The aim of this study was to investigate the effect of firing cycle on a dental porcelain microstructure in order to correlate microstructure changes with mechanical and thermal properties. A commercial low-fusing dental porcelain powder (Omega 900, Vita) was investigated for this purpose. The powder was treated at different temperatures in the range 750–1000 °C. The fired samples were characterized in terms of their morphology and microstructure, and their mechanical and thermal properties were evaluated.

The results showed that firing temperature affects porcelain microstructure influencing significantly in this way both the mechanical properties and the thermal expansion coefficient of the fired objects. Firing at 800 °C led to a homogeneous structure. After treatment at this temperature, the leucite crystals exhibit their maximum concentration and they are well dispersed into the glassy phase. As a consequence the optimum mechanical strength and the maximum thermal expansion coefficient are observed in these samples.

© 2002 Kluwer Academic Publishers

Introduction

Porcelain-fused-to-metal (PFM) restorations are fabricated by fusing the porcelain to the cast metal substrate at high temperatures, this technique requiring a design of both porcelain and alloy so that they are closely matched in thermal expansion characteristics [1, 2]. The requisite firing and thermal behavior for bonding with dental alloys, as well as the desired esthetics in dental porcelains are obtained by blending, in suitable proportions, glass frits, crystallized glasses, and opaquing and pigmenting oxides [3]. Their structure consists, at room temperature, of tetragonal leucite, a potassium aluminum silicate mineral phase ($K_2O \cdot Al_2O_3 \cdot 4SiO_2$ or $KAlSi_2O_6$), embedded in a feldspar-based glass matrix ($Na_2O-K_2O-Al_2O_3-SiO_2$ system) [2]. These type of porcelains differ in composition and structure from the traditional or tri-axial porcelains, that contain mullite ($3Al_2O_3 \cdot 2SiO_2$) instead of leucite [4].

The mineralogical consistency of the powder as well as the microstructure of the fired porcelain is of great significance for some very decisive thermal and

mechanical properties. The way the porcelain is thermally treated is also a very important factor [5].

The coefficient of thermal expansion, the flexural strength, the modulus of elasticity and the microhardness are some of the properties affected by the microstructure and the thermal processing of these materials [6]. The quality of the properties guarantees the clinical success and the longevity of the final metal–ceramic prosthetic application.

One main factor, playing a significant role in the clinical performance of metal–ceramic restorations, is the linear thermal expansion coefficient (α) of the porcelain, which should be similar to the respective coefficient of the metal substrate onto which the porcelain will be applied. The glass phase that is obtained after the complete melting and cooling of potassium–sodium feldspars ($(Na,K)_2O \cdot Al_2O_3 \cdot 6SiO_2$ or $Na_xK_{1-x}AlSi_3O_8$; $0 < x < 1$) shows no great variation in the value of $\alpha (= 7 \times 10^{-6} \text{ to } 10 \times 10^{-6} \text{ K}^{-1}$; 20–900 °C) [1, 2, 7–9] versus the variations in chemical composition [7]. This value is much lower than the desired thermal expansion

*Author to whom all correspondence should be addressed.

coefficient of the final porcelain. Indeed ceramometallic systems should be deliberately designed with a very small degree of thermal mismatch between the porcelain and the metal substrate. Since in most cases the thermal expansion coefficient of the conventional dental alloys is of the order of 14×10^{-6} – $16 \times 10^{-6} \text{ K}^{-1}$; 100–600 °C [1, 2, 8, 9], it is evident that the applied porcelain should be designed to have a thermal expansion coefficient slightly lower than this value (at about $0.5 \times 10^{-6} \text{ K}^{-1}$ less than the α value of the metal substrate) in order to be kept in a state of compression [9].

The coefficient of thermal expansion of the porcelain can be adjusted by the amount of leucite present in its structure taking into consideration the low thermal expansion of the glassy phase [10]. Leucite has a high coefficient of thermal expansion presenting additionally a polymorphic transformation from the tetragonal to the cubic structure accompanied by a large volume change [6, 11]. The temperature range of the low–high leucite transformation is generally reported to be 605–625 °C with a change of its thermal expansion coefficient at the same time from $\alpha = 11 \times 10^{-6}$ – $13 \times 10^{-6} \text{ K}^{-1}$; 25–600 °C to $\alpha = 20 \times 10^{-6}$ – $25 \times 10^{-6} \text{ K}^{-1}$; 25–625 °C [2, 9, 10]. Mackert *et al.* [12] have found that the transformation of leucite crystallites from the tetragonal to the cubic structure during heating occurs between 400 and 600 °C, while there have been found in the literature values for the lower and upper limits, respectively, of the leucite transformation range as low as 433 to 560 °C, and as high as 684 to 714 °C [10].

Therefore, the role of leucite in dental porcelain expansion is the result of the combination of its inherent high thermal expansion coefficient and its large discontinuous volume change associated with the low–high transformation [10]. It is evident, from the above, that the amount of leucite determines the average thermal expansion coefficient of the porcelain. The softening behavior and the opacity of the porcelain, are also determined by this amount [2, 4].

The leucite content in the porcelain is greatly influenced by its thermal history [13]. It has been shown that the isothermal heat treatment for varying time periods [11, 12], the number of firings [10], or the cooling rate [1] can alter the leucite content modifying the porcelain thermal behavior [12]. Mackert and Evans [14] have described a relationship between thermal expansion and leucite content. For this reason many researchers investigate if possible interferences of leucite crystallization during thermal expansion measurements [15] could induce errors in the thermal expansion coefficient evaluation proposing ways of elimination of the problem [16]. Besides the thermal behavior, the mechanical properties are also affected by the leucite presence [6, 17–22]. It has been reported that an increase in leucite content from 10% to 30% doubles the porcelain flexural strength increasing it from 34.1 to 64.8 MPa [6, 17].

In this study, the microstructure of a newly developed commercial low-fusing porcelain after firing at different temperatures was investigated. The aim of the study was to correlate microstructure changes with porcelain thermal and mechanical behavior after firing. In order that considerable microstructure changes are induced

after the different firing treatments, long dwell time at the firing temperature and slow cooling rate were employed.

Experimental procedure

A commercial low-fusing dental porcelain (Vita Omega 900 Metallkeramik, Dentine, Vita, Zahnfabrik-Bad Säckingen, Germany) was used for this investigation. The porcelain powder before its use was fully characterized. The chemical analysis was carried out by atomic absorption spectrophotometry (Varian Spectra AA.10). The results were confirmed employing an energy dispersive X-ray analysis system (Link ISIS 300 B Detector) attached to a Jeol JSM 6300 scanning electron microscope. The compositions were calculated assuming that the elements Si, Al, K, Na, Ca, Sn, Fe, Ti, Mg and Mn appeared as SiO_2 , Al_2O_3 , K_2O , Na_2O , CaO , SnO_2 , Fe_2O_3 , TiO_2 , MgO and Mn_2O_3 , which are the oxides occurring in porcelains. The particle size distribution of the porcelain powder was measured in a laser particle size analyzer (3600 E, Malvern). The porcelain was characterized in terms of its behavior during thermal treatment by means of Differential Thermal Analysis (Setaram TGA-DTA 92 16. 18 system). The measurement was carried out in air employing a heating rate of 2 °C/min in a Pt crucible.

The porcelain powder, after the characterization studies, was shaped into cylindrical rods (length, 55.0 mm; diameter, 5.0 mm). The shaping was performed using a piston extruder properly adjusted to an Instron 8562 mechanical testing machine. The extruded dental porcelain rods were treated at different temperatures in the range of 750–1000 °C in a special laboratory oven. Both the firing and the cooling rate were 300 °C/h, while the dwell time at the final temperature was 2 h. After firing, the porcelain rods were characterized in terms of their physicochemical and mechanical properties. The crystal structure of the as prepared dental porcelain rods was studied by X-ray diffraction analysis (Siemens D500 X-ray diffractometer, CuK_α radiation). The structure was identified on the basis of the d values given by the ASTM diffraction data files.

The bending strength of the rods was measured at a four-point bending test system fitted in an Instron 8562 mechanical testing machine. Six specimens were employed for each measurement, while bending was conducted at a crosshead speed of 1 mm/min. Bending test measurements were followed by microhardness evaluation at a proper hardness tester system (Jena Jenavert, Model MHP 160-Microhardness Tester). Additionally, the fired porcelains were characterized in terms of their morphology at scanning electron microscopy (Jeol, JSM-6300) by employing secondary electron images. Finally, the thermal expansion coefficient of these samples was evaluated in a Netzsch dilatometer (DIL 402 C). The measurements were carried out in air with a heating rate of 5 °C/min.

Results and discussion

The results of chemical analysis confirmed that the porcelain under investigation has the typical composition of conventional dental porcelains, that is, SiO_2 , 60%;

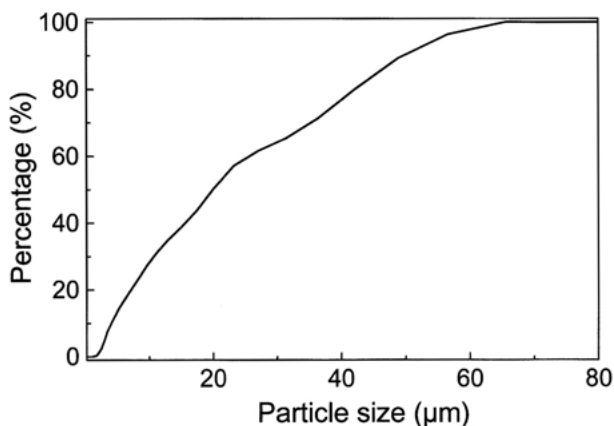


Figure 1 Particle size distribution of the porcelain powder.

Al_2O_3 , 16.5%; K_2O , 7% and Na_2O , 5%, while smaller quantities of other oxides such as CaO , TiO_2 , MgO , SnO_2 were detected.

Particle size analysis on the porcelain powder proved that it is a fine grained one exhibiting a narrow particle size distribution (Fig. 1) with sizes in the range 50–4 μm . Indeed, as it can be seen in Fig. 1, 90% of the porcelain powder particles have a characteristic diameter smaller than 50 μm , while 10% of them are smaller than 14 μm .

The differential thermal analysis results are shown in Fig. 2. As it is seen in the diagram, an endothermic phenomenon takes place between 639 and 854 $^{\circ}\text{C}$ presenting a peak at 740 $^{\circ}\text{C}$. This phenomenon can be attributed to the glass transition of the porcelain. A second and sharper endothermic phenomenon starting at about 1040 $^{\circ}\text{C}$ and continuing above 1200 $^{\circ}\text{C}$ (the end temperature of the measurement) corresponds to the porcelain melting. These results suggest that the examined dental porcelain is a low-fusing one, requiring a firing temperature higher than 750 $^{\circ}\text{C}$ in order that vitrification takes place.

The phase composition of the porcelain, before and after firing, was investigated employing X-ray diffraction analysis. The X-ray patterns obtained from the as received powder as well as from the fired porcelain samples after their firing at 800, 850, 900, 950 and

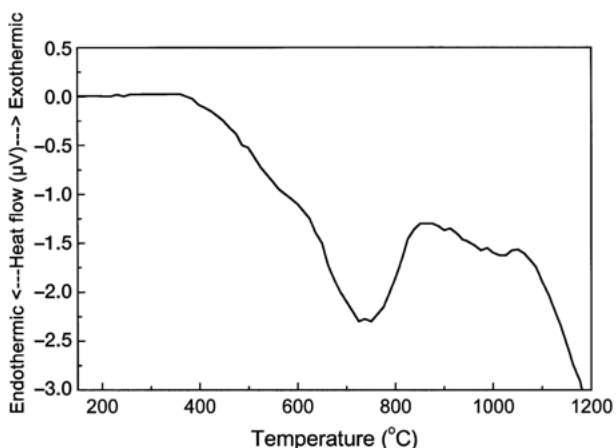


Figure 2 Differential thermal analysis of the porcelain powder.

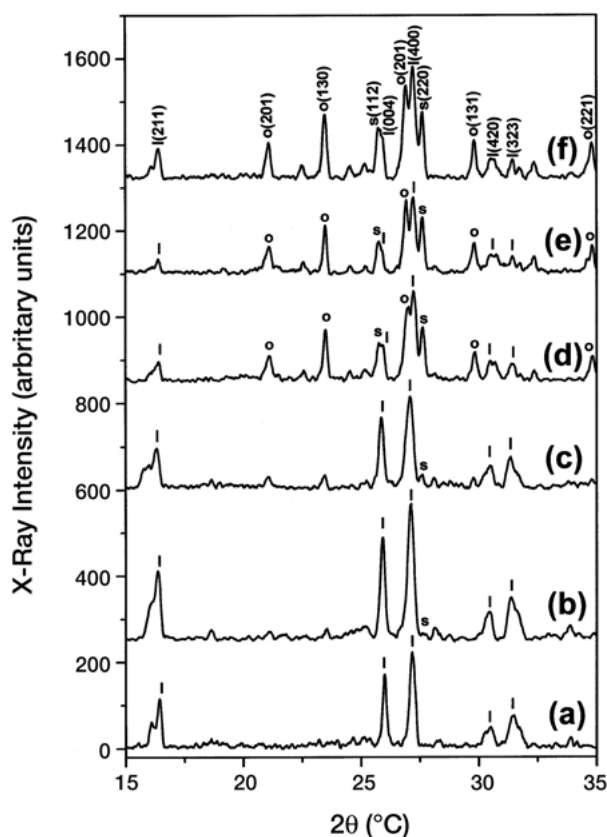


Figure 3 X-ray diffraction patterns of the porcelain samples: (a) untreated, (b) fired at 800 $^{\circ}\text{C}$, (c) fired at 850 $^{\circ}\text{C}$, (d) fired at 900 $^{\circ}\text{C}$, (e) fired at 950 $^{\circ}\text{C}$, (f) fired at 1000 $^{\circ}\text{C}$.

1000 $^{\circ}\text{C}$ are presented in Fig. 3(a)–(f) respectively. In these figures the crystallographic planes at which the X-ray diffraction occurs are also written above the corresponding peaks.

The X-ray pattern of the as received porcelain before any treatment (Fig. 3(a)) presents the typical appearance of a glassy phase in which the only crystalline phase that can be detected is leucite. No significant changes were found in the XRD patterns of the porcelain samples after firing at 750 and 775 $^{\circ}\text{C}$. The same appearance is also observed in the pattern of the sample fired at 800 $^{\circ}\text{C}$ (Fig. 3(b)). However, an increase in leucite peaks intensity is easily noticeable in this case. Additionally, after firing at this temperature, very small peaks of sanidine can be hardly identified for the first time. As firing temperature increases furthermore, the leucite peaks intensity presents a small decrease up to the temperature of 950 $^{\circ}\text{C}$ (Fig. 3(c)–(f)), while on the contrary sanidine content increases continuously up to the firing temperature of 875 $^{\circ}\text{C}$. After firing at 900 $^{\circ}\text{C}$, another phase, orthoclase, can also be identified (Fig. 3(d)).

These changes in microstructure can be more easily observed in Fig. 4 where the surface area of the main peaks of the different phases present in the structure are plotted versus the firing temperature. Various researchers have proved that the peak area of the main leucite peak detected in dental porcelains can be employed successfully to determine quantitatively the leucite content in the porcelain samples [6, 8, 10]. In the present study, the peak areas were employed only to represent schematically the trend in leucite content changes during the

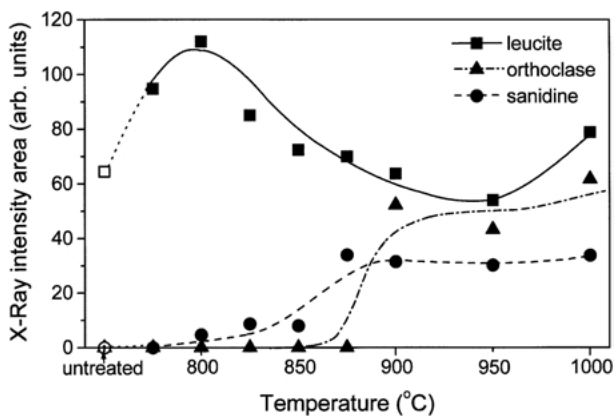


Figure 4 X-ray intensity area of the main peak of the different phases present in the porcelain structure after firing at different temperatures.

different thermal treatment procedures. Observing Fig. 4, as already discussed, an initial increase of leucite content as the firing temperature rises to 800 °C can be seen. On the contrary, for treatment at higher temperatures a continuous decrease of the leucite peak area up to the temperature of 950 °C is observed. However, after firing at 1000 °C, the leucite peak area, measured in the respective samples, is found to increase again. A new phase, sanidine, is detected after these treatments. The first traces of sanidine are hardly detectable at 800 °C, while as the firing temperature increases, sanidine peak area increases constantly up to the temperature of 875 °C, remaining constant at this level for treatment at higher firing temperatures.

Modifications of leucite content in the dental porcelains due to the thermal treatment procedure (multiple firings, isothermal annealing at lower temperatures after firing, cooling rate etc.) have been reported by several researchers [1, 10–12]. Many of these researchers [2, 10, 12], in light of the ternary $K_2O-Al_2O_3-SiO_2$ diagram discuss that for ordinary dental porcelain compositions, leucite is not an equilibrium phase. They point out that studying this diagram, liquid, leucite plus liquid, leucite plus sanidine plus liquid, sanidine plus liquid, sanidine are the equilibrium phases in descending order of temperature [2]; thus sanidine is the stable phase at room temperature. These transformations are reconstructive ones and therefore sluggish and irreversible. For this reason, some high-temperature structures are quenchable as metastable phases [2]. The equilibrium reactions occurring and the respective suggested temperatures are:



where CL, S and L denote the cubic leucite, sanidine and liquid respectively.

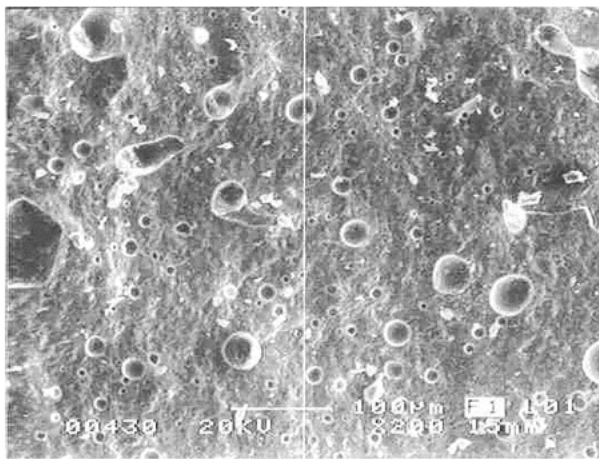
The kinetics of these reconstructive transformations (the precipitation of sanidine and the dissolution of leucite) were studied by Bareiro and Vicente [2] who performed isothermal annealing of a typical PFM porcelain at different temperatures in the range 800–1000 °C for different time periods. Their conclusion was

that the maximum precipitation rate of sanidine occurs at about 900 °C, while the maximum extinction rate of cubic leucite is tentatively located at 850–900 °C. A short thermal treatment time period of 20 min is required for sanidine precipitation to be completed at 900 °C, while a long period of 700 min is required for the leucite extinction at its maximum extinction rate temperature. Other researchers have also detected the appearance of sanidine after prolonged firing at 800 and 900 °C, but not at 1100 °C [1], while after multiple firings of very short time periods, sanidine could be observed only after firing at the elevated temperature of 970 °C.¹⁰ On the contrary, it is reported that isothermal annealing at the relatively low temperature of 750 °C can lead to the increase of leucite content [10, 11].

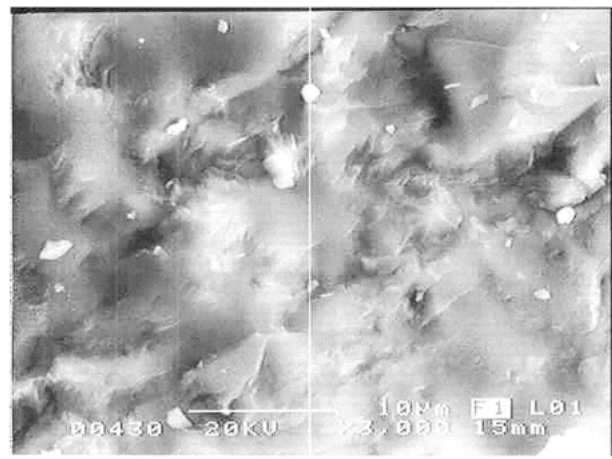
The results obtained in the present work are very consistent with the results of the studies in the literature. Indeed, firing at low temperatures caused the increase of leucite as reported by Mackert *et al.* [10, 11]. Moreover, the lowest leucite content was observed at 950 °C, while a continuous decrease of leucite is detected from a temperature of 800 °C and above (Fig. 4). The difference in the temperature of maximum leucite dissolution between this work (950 °C) and the work of Bareiro and Vicente [2] (850–900 °C) could be justified by the fact that in the present work the porcelain samples were fired for a smaller time period (120 min) compared to the time required for the leucite dissolution (700 min) in the study of Bareiro and Vicente [2]. However, the maximum sanidine content was observed at 875 °C, a temperature, which is in perfect agreement with the results of these researchers. Firing at higher temperatures does not change the sanidine content, which is kept constant and equal to the value measured after firing at 875 °C.

An additional phase, orthoclase, was detected in the samples fired at the temperature range 900–1000 °C. The slow cooling rate in combination with the increased amount of liquid phase formation (reactions 1 and 2) at these elevated firing temperatures permitted the crystallization of some part of the liquid to this phase during cooling. The SEM pictures and the thermal expansion coefficient curves, which are discussed below confirmed also the enhanced degree of crystallization in the samples fired at this temperature range.

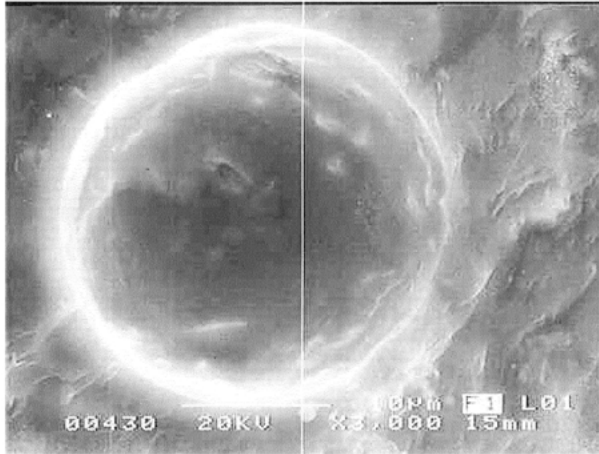
The microstructure of the fired porcelain was investigated under the scanning electron microscope. Typical SEM photographs under different magnifications of a fractured surface of the porcelain sample after firing at 800 °C can be seen in Fig. 5. At the low magnification of 200 times (Fig. 5(a)), a flat glassy area can be observed in which crystals gathered into groups are embedded. Indeed, magnifying (3000 times) an area exhibiting such a crystal group (Fig. 5(b)), crystals, most probably of leucite, according to XRD analysis, with dimensions of about 1- μ m or less surrounded by the glassy phase are revealed. Fig. 5(c) presents a high magnification (3000 times) of the flat glassy region, proving the complete vitrification of the structure and its glassy appearance. Very small pores with a mean diameter in the submicron range are very sparsely observed in it. However, observing carefully the glassy phase, crystallized regions such as that of Fig. 5(d) (magnification 10 000 times)



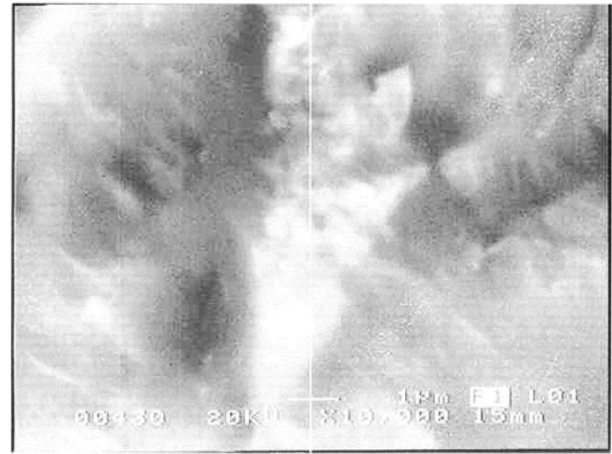
(a)



(b)



(c)



(d)

Figure 5 Typical SEM pictures of the fractured surface of a porcelain sample fired at 800 °C under different magnifications: (a) 200 ×, (b) 3000 ×, (c) 3000 ×, (d) 10000 ×.

with crystal dimensions less than 300 nm can be hardly detected.

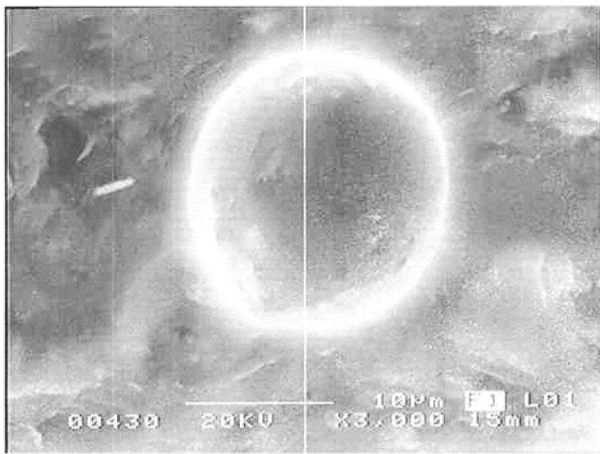
Fig. 6 depicts the fractured surface structure after firing at 775 °C (Fig. 6(a)–(c)) and 825 °C (Fig. 6(d)). The structure of the samples fired at 775 °C is quite similar to that of the samples fired at 800 °C, although leucite crystals could not be distinguished at the respective areas (Fig. 6(a)), perhaps due to their very small size in this case. Another difference is that crystallized areas within the glassy phase are more easily detected (Fig. 6(b)). These areas are comprised of crystals with dimensions in the order of 100 nm as shown in Fig. 6(c). The porosity in the glassy phase, in this case, is also too low with the pores being again in the submicron range (Fig. 6(b), (c)). On the contrary, in the case of the samples fired at 825 °C, the porosity in the glassy phase is presented slightly increased with larger pores (Fig. 6(d)), while complete vitrification is observed.

After firing at 850 °C (Fig. 7), the porcelain presents a higher degree of crystallization. The crystals can be easily distinguished in this case (Fig. 7(a)–(c)), while some new elongated grains, probably of sanidine according to XRD studies, have been developed in the vicinity of leucite crystals. These crystals, exhibiting a

needle-like appearance, have a mean length of the order of 4 µm and are clearly gathered into groups. The porosity in the glassy phase (Fig. 7(d)) is further increased and the pore diameters reach values up to 3 µm.

The crystallization phenomenon is much more intense after firing at 875 °C as it can be seen in Fig. 8. Leucite and sanidine crystals are gathered into large agglomerates (Fig. 8(a)) making their distribution quite inhomogeneous. As it was discussed when analyzing the XRD results, this temperature is the temperature where the maximum formation rate of sanidine occurs. The SEM studies confirmed this phenomenon. Sanidine crystals have been enlarged in both dimensions reaching 6 µm in length (Fig. 8(b),(c)). They present distinct boundaries with quite large pores (with diameters in the range of 2–5 µm) among them (Fig. 8(c)). The glass phase in this case exhibits many small pores (most of them in the submicron range) as a result of the rearrangement due to the rapid reaction of the liquid phase with leucite and sanidine (reaction 2).

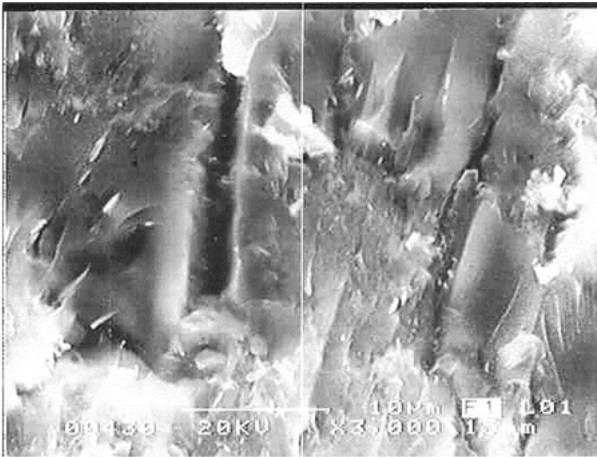
After firing at 900 °C (Fig. 9) the microstructure remains almost the same as in the previous case. However, the crystal agglomerates have been further enlarged making the crystal phase inhomogeneously dispersed into the glassy one (Fig. 9(a)). Sanidine



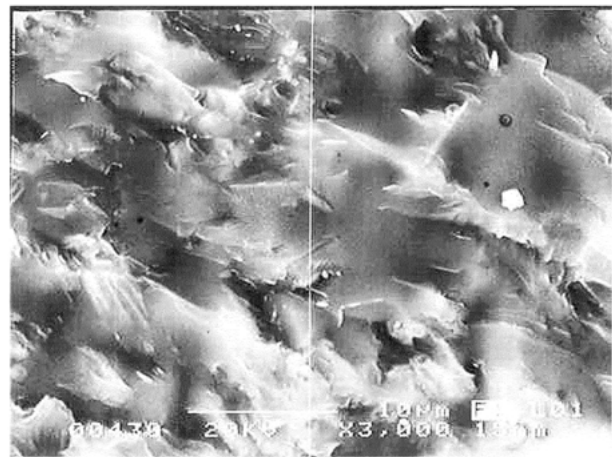
(a)



(b)



(c)



(d)

Figure 6 Typical SEM pictures of the fractured surface of a porcelain sample fired at 775 °C under different magnifications: (a) 3000 ×, (b) 3000 ×, (c) 10000 ×; (d) fractured surface of a porcelain sample fired at 825 °C, magnification 3000 ×.

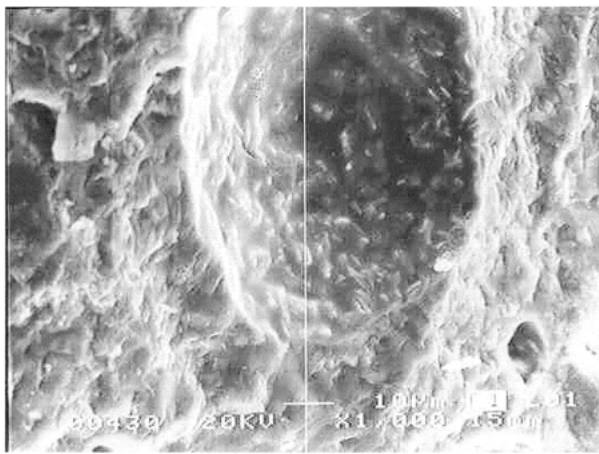
crystals have been further enlarged reaching almost 10 µm in length (Fig. 9(b)), while spherical leucite crystals of 1 µm in diameter gathered into groups are distinguished among them (Fig. 9(c)). Porosity exists in the grain boundaries, with pore sizes approaching 10 µm. The glassy phase contains also micropores, but the porosity is less compared to that observed in the sample fired at 875 °C.

The thermal expansion coefficient curves of the fired porcelain samples, after firing at different temperatures (775, 800, 825, 850 and 875 °C), are shown in Fig. 10. All the curves are almost similar. Observing these curves, the conclusion is that they present many similarities with the typical thermal expansion curve of a glassy phase [23] in which a crystal phase is embedded. This curve presents a slow increase in the expansion coefficient up to a temperature which represents the onset of the glass transition (T_{onset}), followed by a sudden increase up to a temperature called softening point (T_s), which represents the end of the glass transition phenomenon. Above this temperature a very steep decrease corresponding to viscous flow of the sample is observed. Indeed, in the experimental curves, the thermal expansion coefficient increases progressively from room temperature up to the onset of the glass transition,

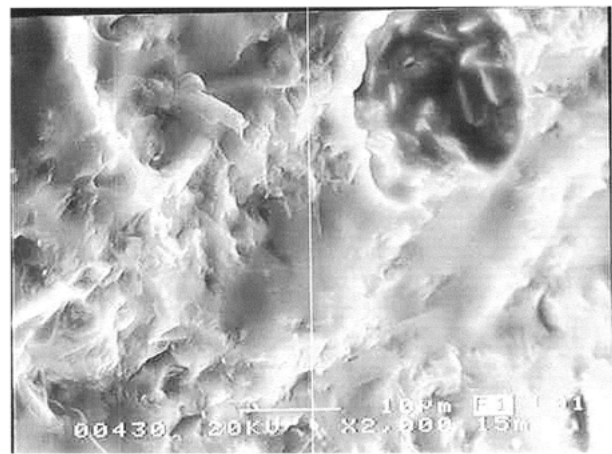
showing its maximum value at the softening point. Further heating to higher temperatures above the glass transition area, leads to the decrease of the thermal expansion coefficient.

However, it is worth noting that both the onset glass transition temperature and the softening point depend on the temperature at which the porcelain sample had been previously sintered. As this temperature increases from 800 to 875 °C, the glass transition temperature decreases constantly from 524 to 516 °C, while the softening point shows a greater shift decreasing from 605 to 550 °C. The only exception to this behavior is the sample previously fired at 775 °C, which exhibits slightly lower glass transition temperature than that of the sample fired at 800 °C.

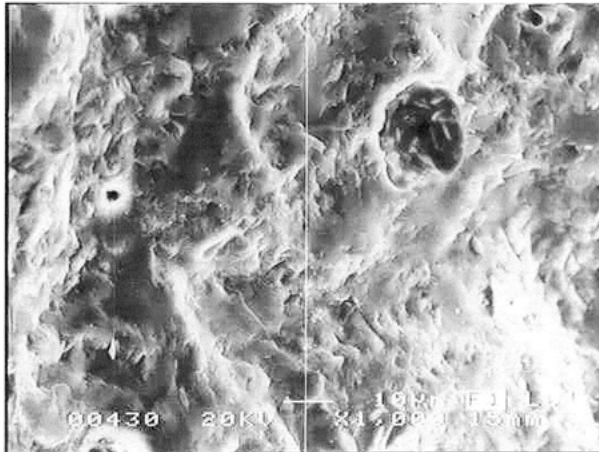
This phenomenon can be explained by the differences observed in the microstructure after the different thermal treatments: (a) the decrease of leucite content by the firing temperature rising in the range 800–875 °C, and (b) the increase of crystallization degree at the same time due to sanidine and orthoclase formation. The softening behavior dependence of dental porcelains on their leucite content [4] is also reported in the literature. Another observation that can be made looking at the dilatometric curves is the less viscous behavior above the softening



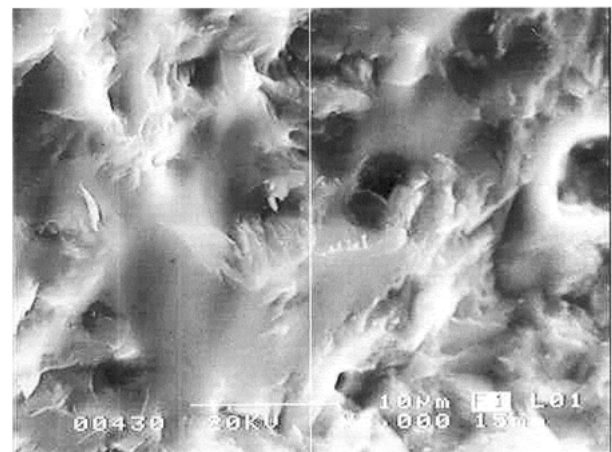
(a)



(b)



(c)



(d)

Figure 7 Typical SEM pictures of the fractured surface of a porcelain sample fired at 850 °C under different magnifications: (a) 1000 ×, (b) 1000 ×, (c) 2000 ×, (d) 3000 ×.

point for the samples fired at higher temperatures, which proves their higher degree of crystallization confirmed by the XRD analysis and the SEM studies.

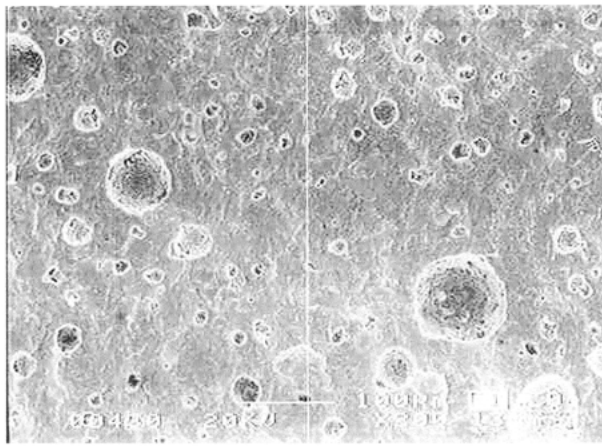
The glass transition temperature range is of high significance for the porcelain that is going to be applied and used as a dental restorative material. The thermal expansion coefficient of the porcelain at this temperature area should match that of metal substrate for successful metal–ceramic constructions. As it can be seen, observing the thermal expansion curves in Fig. 10, the thermal expansion coefficient values depend also on the firing treatment in exactly the same way as the glass transition temperature. A clear shift of the thermal expansion curve to higher values can be observed as the sintering temperature of the porcelain samples increases from 775 to 800 °C, while for higher temperatures the curves are shifted to progressively lower values.

In Fig. 11 the thermal expansion coefficient values at the glass transition temperature are plotted versus the firing temperature of the porcelain. The coefficient ranges between 13.1×10^{-6} and $15.9 \times 10^{-6} \text{ K}^{-1}$ showing the same behavior: increase up to 800 °C and successive decrease. Thus, the maximum value ($15.9 \times 10^{-6} \text{ K}^{-1}$) was measured on the porcelain fired at 800 °C. This behavior follows exactly the leucite curve

in Fig. 4 permitting its attribution to leucite content variations. Indeed, as discussed previously, the leucite crystallization increases by firing up to 800 °C, decreasing for higher firing temperatures due to reaction towards sanidine and liquid phase.

In fact, studies in the literature have shown that the thermal expansion coefficient of dental porcelains is directly related to their leucite content [3, 14]. As discussed in the introduction, the leucite thermal expansion coefficient in the temperature range of interest (20–600 °C) is of the order of 20×10^{-6} – $25 \times 10^{-6} \text{ K}^{-1}$. This high value affects significantly the thermal expansion coefficient of the porcelain since the glassy phase has a much lower thermal expansion coefficient ranging at about $7 \times 10^{-6} \text{ K}^{-1}$ (20–900 °C). In contrast to leucite, sanidine does not have any influence on the thermal expansion behavior since its coefficient is at 4×10^{-6} – $8 \times 10^{-6} \text{ K}^{-1}$, i.e. very close to that of the glassy phase [2].

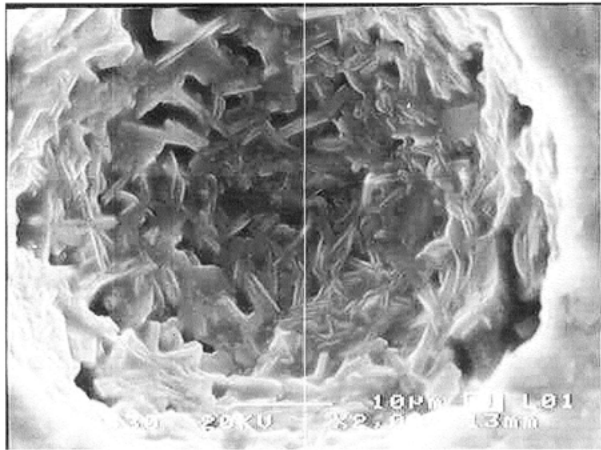
The results of the strength experiments concerning both the modulus of rupture and the modulus of elasticity are summarized in Fig. 12(a), and (b) respectively. In both cases, the diagrams exhibit a maximum value for the samples fired at 800 °C, while at 750 °C the strength is



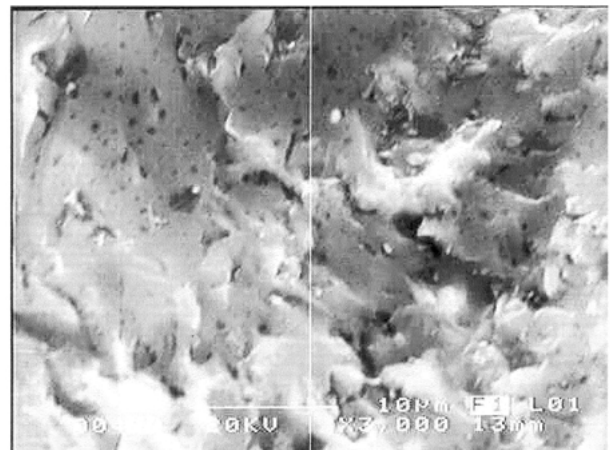
(a)



(b)



(c)



(d)

Figure 8 Typical SEM pictures of the fractured surface of a porcelain sample fired at 875 °C under different magnifications: (a) 200 ×, (b) 2000 ×, (c) 5000 ×, (d) 3000 ×.

negligible. Firing at 900 °C caused deformation on the porcelain samples due to melting initiation making the measurement of their mechanical strength impossible. The maximum values of strength obtained at 800 °C, can be attributed to the complete vitrification which occurred at this temperature accompanied by the lack of porosity, the maximum leucite content achieved and the quite homogeneous dispersion of leucite crystals into the glassy phase. It is worth noting that the maximum strength was observed at exactly the same temperature where the maximum leucite content was detected. Although, at higher temperatures the crystallization phenomenon was extended with the sanidine and orthoclase formation, the inhomogeneities in crystal dispersion along with the grain size growth and the creation of porosity into the glassy phase due to the rapid reactions occurring have caused significant deterioration in the mechanical properties. The importance of the presence of leucite crystallites has been long recognized by the researchers as a factor enhancing significantly the mechanical properties of the dental porcelains, since they can prevent the microcracks propagation [17–22].

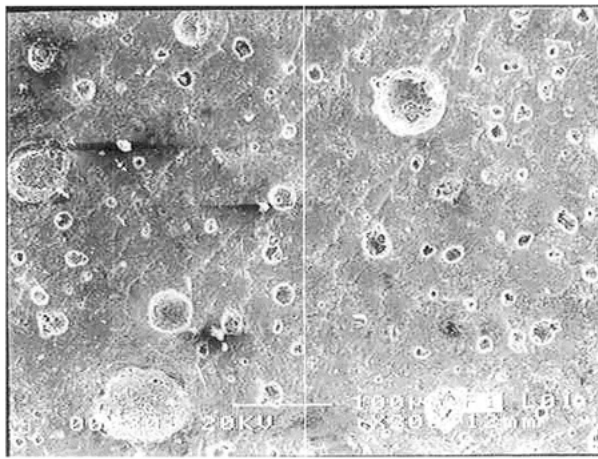
Microhardness studies on the fired porcelain samples indicated exactly the same behavior for microhardness as that observed in the bending strength measurements (Fig.

12(c)). In this case as well, the maximum value was observed after firing at 800 °C and it was of the order of 382 kg/mm².

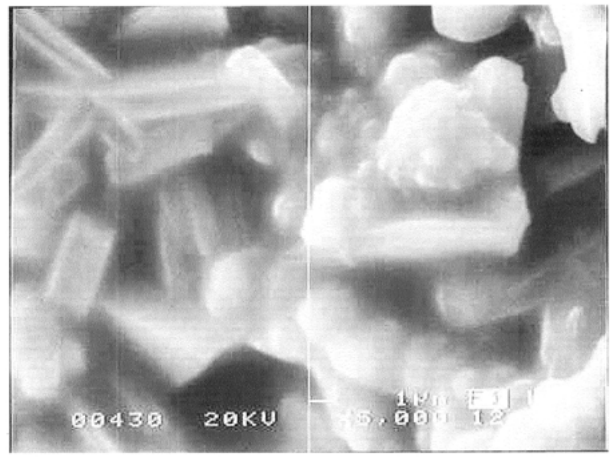
Finally, it is worth noting that both the thermal expansion coefficient and the mechanical properties show their maximum values after firing at 800 °C, the temperature where leucite content maximizes, while the reaction rate of leucite dissolution to sanidine and liquid is too low to permit the creation of inhomogeneities and porosity in the structure. It must be pointed out at this point that this study concerned prolonged firing time at each temperature investigated and slow cooling rates in order to permit detectable differences in microstructure to occur, since the aim was the correlation of microstructure with properties.

Conclusions

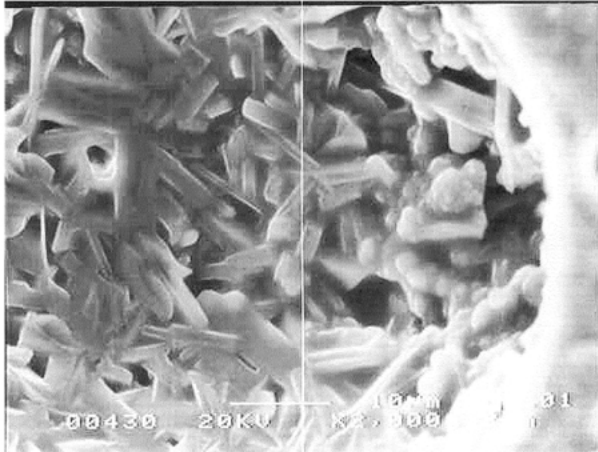
- The firing temperature of the porcelain affects significantly its microstructure influencing directly, in this way, both mechanical and thermal properties.
- The optimum mechanical properties of the porcelain were observed after firing at 800 °C. In the



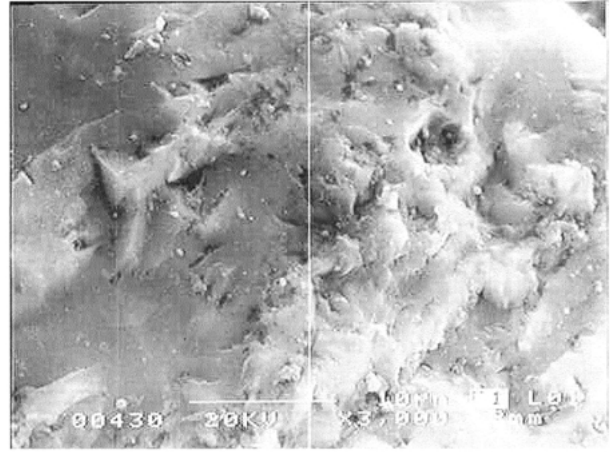
(a)



(b)



(c)



(d)

Figure 9 Typical SEM pictures of the fractured surface of a porcelain sample fired at 900 °C under different magnifications: (a) 200 ×, (b) 2000 ×, (c) 5000 ×, (d) 3000 ×.

samples treated at this temperature, the maximum leucite peaks were detected by XRD, while, as confirmed by SEM investigation, complete vitrification was achieved, with the leucite crystals being homogeneously dispersed within the glassy matrix.

- Firing at higher temperatures results in leucite crystals growth, favoring at the same time leucite dissolution to sanidine and the creation of porosity.

Additionally, the leucite and sanidine crystals begin to agglomerate and in this way their homogeneous dispersion into the structure is reduced. All these factors influence the mechanical properties negatively.

- Both the glass transition temperature and the thermal expansion coefficient depend also on the firing treatment exhibiting the highest values after firing at 800 °C, the temperature where the

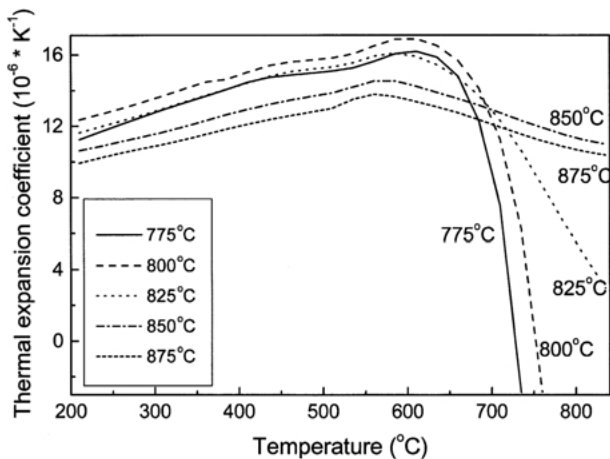


Figure 10 Thermal expansion coefficient curves of the porcelain samples fired at different temperatures.

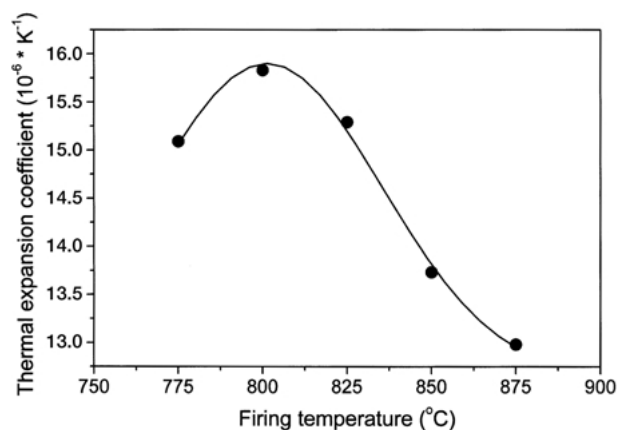
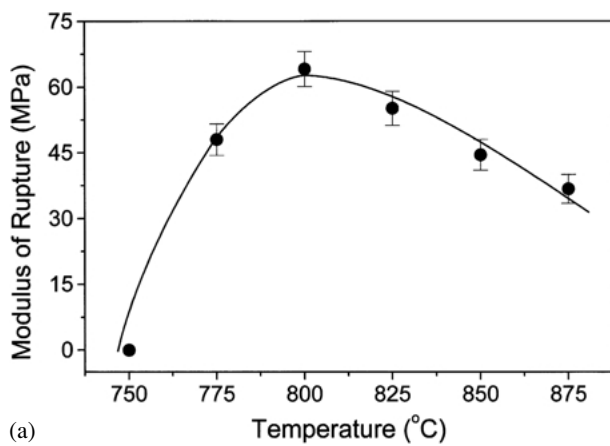
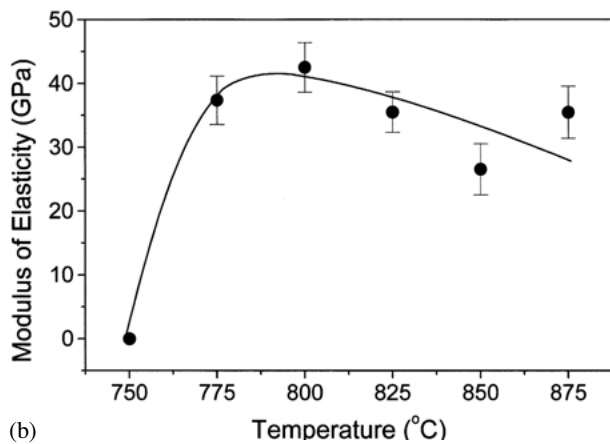


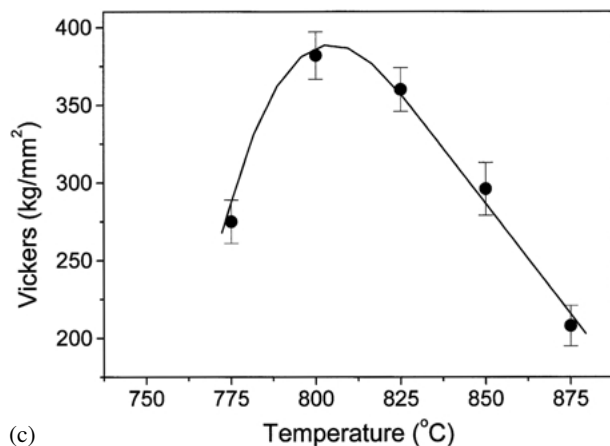
Figure 11 Thermal expansion coefficient of the porcelain samples at their glass transition temperature versus the firing temperature.



(a)



(b)



(c)

Figure 12 Mechanical properties of the porcelain samples versus the firing temperature: (a) modulus of rupture, (b) modulus of elasticity, (c) Vickers microhardness.

maximum leucite content was detected and the optimum microstructure and mechanical properties were observed.

References

1. J. R. MACKERT and A. L. EVANS, *J. Dent. Res.* **70**(5) (1991) 137.
2. M. M. BARREIRO and E. E. VICENTE, *J. Mater. Sci.: Mater. Med.* **4** (1993) 431.
3. J. R. MACKERT, M. B. BUTTS, G. M. BEAUDREAU, C. W. FAIRHURST and R. H. BEAUCHAMP, *J. Dent. Res.* **64**(9) (1985) 1170.
4. C. HAHN, "Ceramic Monographs, Handbook of Ceramics, Dental Porcelain" (Verlag Schmid GmbH, Feiburg, 1981) p. 1.
5. T. R. PAPADOPOULOS, A. TSETSEKOU and D. ANDRITSAKIS, *Balk. Stomatol. J.* **3** (1999) 146.
6. J. L. ONG, D. W. FARLEY and B. K. NORLING, *Dent. Mater.* **16** (2000) 20.
7. P. J. VERGANO, D. C. HILL and D. R. UHLMANN, *J. Am. Ceram. Soc.* **67**(1) (1967) 59.
8. P. W. PICHE, W. J. O'BRIEN, C. L. GROH and K. M. BOENKE, *J. Biomed. Mater. Res.* **28** (1994) 603.
9. J. A. HAUTANIEMI, and H. HERØ, *J. Am. Ceram. Soc.* **74**(6) (1991) 1449.
10. J. R. MACKERT and A. L. EVANS, *ibid.* **74**(2) (1991) 450.
11. J. R. MACKERT, S. W. TWIGGS and A. L. EVANS-WILLIAMS, *J. Dent. Res.* **74**(6) (1995) 1259.
12. J. R. MACKERT, B. M. BUTTS, R. MORENA and C. W. FAIRHURST, *J. Am. Ceram. Soc.* **69** (1986) 69.
13. C. W. FAIRHURST, D. T. HASHINGER and S. W. TWIGGS, *J. Dent. Res.* **68**(9) (1967) 1313.
14. J. R. MACKERT and A. L. EVANS, *ibid.* **71** (1992) 238, Abstract No. 1060.
15. J. R. MACKERT, S. S. KAJOTIA, C. M. RUSSELL and A. L. WILLIAMS, *Dent. Mater.* **12** (1996) 8.
16. S. S. KAJOTIA, J. R. MACKERT, S. W. TWIGGS, C. M. RUSSELL and A. L. WILLIAMS, *ibid.* **15** (1999) 390.
17. S. KADIMISETTY and M. ROSENBLUM, *J. Dent. Res.* **77** (1992) 7, Abstract No. 523.
18. M. KON, F. KAWANO, K. ASAKA and N. MATSUMOTO, *Dent. Mater. J.* **13**(2) (1994) 138.
19. P. S. BAKER and A. E. CLARK, *Int. J. Prosthodont.* **6** (1993) 291.
20. S. KARLSSON, M. MOLIN and T. MYRVOLD, *Acta Odontol. Scand.* **52** (1994) 290.
21. S. S. SHERRER, J. R. KELLY, G. D. QUINN and K. XU, *Dent. Mater.* **15** (1999) 342.
22. J. L. DRUMMOND, T. J. KING, M. S. BAPNA and R. D. KOPERKI, *ibid.* **16** (2000) 226.
23. W. D. KINGERY, H. K. BOWEN and D. R. UHLMANN, "Introduction to Ceramics", 2nd edn (A Wiley-Interscience Publication, New York, 1973) p. 92.

Received 21 September 2000
and accepted 24 July 2001